MANUSCRIPT COVER PAGE

Beam Interactions with Materials and Atoms
Nuclear Instruments and Methods in Physics Research, Section B.

Paper Reference Number : Abstract #ID: _102_

Title of Paper: Combining Dynamic Modelling Codes with Medium Energy Ion Scattering Measurements to Characterise Plasma Doping

Corresponding Author :Jonathan England
Telephone :+44 7742 161 721
Fax :
E-mail :jonathan_england@amat.com

Manuscript Length Estimation Table

Number of characters[1] (using "character count")	**13196**	**= A**
Number of 1-column tables or figures[2]		**= B**
Number of 2-column tables or figures[2]	**4**	**= C**

Estimated number of printed pages = (A + 1300B + 5000C)/8500	**3.9**

[1] Including title, abstract, captions and references, including spaces.
[2] Each independent figure including Fig.a, Fig.b, Fig.c, etc. must be counted separately.

Combining Dynamic Modelling Codes with Medium Energy Ion Scattering Measurements to Characterise Plasma Doping

J. England[a] , W. Möller[b], J. A. van den Berg[c], A. Rossall[c], W.J. Min[d] and J. Kim[d]

[a]*Varian Semiconductor Equipment, Silicon Systems Group, Applied Materials Inc., USA*

[b]*Helmholtz-Zentrum Dresden-Rossendorf, Institute of Ion Beam Physics and Materials Research, Bautzner Landstrasse 400, 01328 Dresden, Germany*

[c]*International Institute for Accelerator Applications, School of Computing and Engineering, University of Huddersfield, Huddersfield, HD1 3DH, UK.*

[d]*Korea Materials and Analysis Corporation, Daejon 305-500, South Korea*

Abstract

Plasma doping ion implantation (PLAD) is becoming increasingly important in the manufacture of advanced semiconductor device structures but a fundamental understanding of PLAD is complicated. A model of PLAD into planar substrates has been constructed using the one dimensional computer code TRIDYN to predict collision cascades and hence substrate compositional changes during implantation. Medium Energy Ion Scattering (MEIS) measurements of dopant profiles in PLAD processed samples were used to calibrate the input ion and neutral fluxes to the model. Rules could then be proposed for how post implant profiles should be modified by a cleaning step. This learning was applied to a three dimensional TRI3DYN based model for PLAD implants into FinFET like structures. Comparison of the model to dopant profile measurements made by time of flight (TOF)-MEIS revealed the angular distributions of neutral species and doping mechanisms acting in three dimensional structures.

Keywords: ion-implantation, ion beam modelling, TRIDYN, TRI3DYN, plasma doping, PLAD, FinFET

[*]***Corresponding author:*** Dr Jonathan England: *jonathan_england@amat.com*

1. Introduction:

Plasma doping ion implantation (PLAD) is becoming increasingly important in enabling the manufacture of advanced semiconductor devices. PLAD is simple in concept: a negatively biased substrate immersed in a plasma is doped by ions and neutrals from that plasma. However, a fundamental understanding of PLAD is complicated because high fluence implantation, deposition, sputtering and ion beam mixing have to be taken into account during the implant after which additional passivation, cleaning and annealing steps have to be considered. The fluxes and compositions of neutral species that deposit on the substrate surface during PLAD cannot be directly measured and although the ions can be counted in a Faraday detector placed around the wafer, their compositions are unknown. The measurement of post PLAD dopant profiles should allow the neutral and ion compositions and fluxes to be determined but such profiles are difficult to measure. Profiling methods such as Secondary Ion Mass Spectroscopy and Dynamic x-ray Photoelectron Spectroscopy suffer from sputter mixing and matrix dependent effects unlike Medium Energy Ion Scattering which can readily yield absolute numbers of dopant atoms. This study reports how the interpretation of MEIS profile measurements was helped significantly by using TRIDYN [1], an established, one dimensional, dynamic code that modelled substrate evolution during implantation by calculating collision cascades using the binary collision approximation.

The angular distributions of arriving ions and neutral species does not greatly influence dopant profiles produced in planar substrates, but can affect the doping of 3D structures. Ions, accelerated across the plasma sheath, arrive in a direction normal to the wafer surface. Neutral atoms originating from the background gas can be modelled with cosine angular distributions, but neutrals originating from other sources, such as chamber walls, can have different angular distributions. In this study, PLAD dopant profiles in FinFET like structures were measured using

a TOF-MEIS system. TRI3DYN [2] is a newly developed, three dimensional version of TRIDYN, in which collision cascades initiated by particles, whose incident angular distributions can be varied, are also calculated using the binary collision approximation. The three dimensional substrate is described by voxel elements which are changed throughout the model as a result of the injected ions, sputtered atoms and collision cascade mixing. Results from TRI3DYN models were compared to the MEIS dopant profile measurements and TEM images to give information on neutral species angular distributions and indicated implantation mechanisms occurring during PLAD processes.

2. PLAD Process

Bare silicon wafers, biased at 7keV, were implanted with arsenic in a VIISta PLAD system [3] in Gloucester, MA using a plasma generated from a gas mixture of 5% AsH_3 in H_2 to a total ion fluence of $1x10^{16}cm^{-2}$. Wafers patterned with features that included 110nm pitch, 130nm tall FinFETs like structures were PLAD implanted with arsenic from a mixture of 5% AsH_3 in Xe/H_2 at a bias of 2keV to a total ion fluence of $5x10^{15}cm^{-2}$. Although this study did not involve pre-implant lithography steps, the samples underwent an industry standard SPM (sulphuric acid hydrogen peroxide mixture) wet chemical clean in a Nexgen Technologies wet bench to represent the production step of photo-resist removal. Following a "spike" anneal (1050°C held for 1.7s) in a nitrogen atmosphere in a Mattson AST 3000 annealer, a dilute hydrofluoric (DHF) acid step was used to remove surface oxide.

3. Dopant Profile Metrology

MEIS measurements on planar wafers were carried out on the University of Huddersfield MEIS system [4] using 100keV He^+ ions and a scattering angle of 90°. Double aligned spectra were collected for He ions directed at a 54.7° entrance angle along the [-1 -1 1] channel direction and exiting along the [1 1 2] blocking direction. The samples were tilted for a 61.7° entrance angle

and also twisted by 7° when collecting random orientation spectra, examples of which are shown in Figure 1.

The FinFET structures were measured by Korean Materials and Analysis Corporation using their TOF-MEIS system [5] which has a sample imaging capability and small primary beam spot size so that the structures contained in a square die of 250μm side could be measured. 100keV He^+ ions were again used for the primary beam but a 130° scattering angle was used and scattered ions were analysed using a time of flight system rather than a toroidal energy analyser as at Huddersfield. Randomly oriented spectra were taken for entrance angles of 25° and 65° in a direction twisted 5° away from the normal into the fin sidewalls and with an entrance angle 25° in a direction twisted 5° away from parallel to the fin sidewalls.

Elemental profiles shown in this paper were extracted from MEIS and TOF-MEIS spectra collected from measurements on randomly oriented samples using POWERMEIS [6]. To fit the spectra from planar samples, POWERMEIS trial substrates were divided into layers containing As, Si and O atomic concentrations shown in Figure 2 by the lines and symbols. The layer thicknesses were chosen to be consistent with the TEM images, and choice of layer compositions were guided by the outputs of a TRIDYN model. Atomic concentrations have been reported rather than atomic fractions to help indicate where the layer density is lower than for fully stoichiometric compounds.

To fit spectra from FinFET samples, POWERMEIS substrates were divided into cubic voxels of 2 Angstrom side and simple layers in the fin top, bottom and sidewalls were defined within these voxels. The use of TRI3DYN model outputs as suggestions for 3D POWERMEIS trial solutions (as done for the planar case) has not yet been investigated.

Brightfield TEM images were taken by Evans Analytical Group on parts of planar samples that were coated with Iridium before the TEM lamellae were produced. Energy dispersive spectroscopy (TEM/EDS) measurements were made for some of these samples, but are not discussed further in this paper. Fin samples were first coated with carbon before making the lamellae for brightfield TEM images.

4. Planar PLAD Implant Results

The post implant TEM image of a planar PLAD process is shown in Figure 2a). Ions and neutrals arrived from the left hand side of the image and the original position of the wafer surface before processing was 0 nm. Figure a) shows an amorphous / crystalline interface at +10nm created near the end of range of the As ions. The amorphous layer of uniform contrast from this interface up to the original wafer surface (0nm) consisted of As ions and recoil implanted As neutrals mixed into the Si substrate. The "intermixed layer" between 0nm to -10nm contained As originating from both neutrals and ions from the plasma and Si atoms from the substrate. The TRIDYN model was constructed with assumptions for input fluxes of As ions, As atoms and other neutral species to simulate profiles that matched the measurements. TRIDYN suggested that the amount of Si present in the intermixed layer could not have be due only to Si that had been mixed in from deeper in the substrate, so an additional flux of Si atoms was included in the flux of "other neutral species". This additional Si flux was reasonable because the chamber walls of the PLAD tool had been intentionally coated with a Si rich layer using a pre-conditioning step before any wafers were implanted and sputter products from previously processed wafers will have added to this coating. During implantation, the plasma interacted with the chamber walls to liberate Si and other atoms from the coating which could then deposited onto (or implanted into) the wafer. Hydrogen atoms, deposited as constituents of AsH_x molecules or neutral H radicals, were also included in the TRIDYN model's "other

neutral species" to account for the low density of the intermixed layer. Hydrogen cannot be detected by MEIS of TEM/EDS, so any layer density calculation that considered only the measured atomic fractions of Si and As would have overestimated that density. Furthermore, hydrogen initially deposited onto the wafer could have escaped from the layer to leave voids, further reducing the density. H ions were not considered as they played little role in the ion beam mixing processes. The light coloured 2.9nm thick surface layer between -10nm to -12nm in the TEM of Figure 2a) shows a region from which As had effused after the implant, leaving behind Si which had then been oxidised.

The TEM and MEIS data following the wet chemical clean shown in Figure 2b) indicates that almost all of the As had been removed from the intermixed layer above the original wafer surface (now marked by a dark stripe in the TEM image). The Si left behind was oxidised, forming the light coloured 12nm thick oxide layer, less dense than fully stoichiometric SiO_2 (which usually contains $2.3x10^{22}$ Si cm^{-3}). Only As beneath the original substrate surface survived the clean, most of it being recoil implanted As neutrals. In the TRIDYN based model, the clean was simulated by removing As from the intermixed layer above the original surface of the wafer but the Si was fully retained.

The atomic concentrations measured by MEIS were converted to atomic fractions and agreed well with TEM / Energy Dispersion Spectroscopy measurements of these samples (not shown). Further TEM and MEIS measurements made post anneal (not shown) showed recrystallization of the amorphous layer up to the dark line, retention of 80% of the As and survival of the 12nm thick oxide layer which was subsequently removed by DHF.

5. PLAD Implants into FinFETs

Figures 3 and 4 compare a TRI3DYN derived model to the TEM images and TOF-MEIS measurements of PLAD doped FinFETs. The magnitudes of the model's input fluxes were

calibrated from planar measurements of the 5% AsH_3 in Xe/H_2 2keV bias process in the same way described above. The wet clean was assumed to retain all Si but remove As for voxels with Si concentrations below of $3x10^{22}$ cm^{-3}. The figures show the results for the TRI3DYN model in which all the neutrals were all assumed to arrive with normal incidence (characteristic of atoms originating from the chamber walls directly above the sample). This was a better match to the as-implanted TEM than assuming that all the neutrals were gas atoms with a cosine distribution (not shown). The best fit neutral species angular distribution has not yet been determined. Even so, the agreement between the TRI3DYN model and TOF-MEIS is fair, remembering that the model does not include As loss and diffusion during the anneal and that further optimization of the TOF-MEIS spectrum analysis might be possible.

TRI3DYN can illustrate various mechanisms by which PLAD can introduce As atoms into a FinFET sidewall at sufficient depth to survive the wet clean. Figure 5 shows As dopant profiles of a TRI3DYN static model in which a 140nm tall Si fin of 120nm pitch coated with 1nm thick As neutral deposition on all surfaces has been implanted with equal numbers of As and Xe ions at 2keV to a fluence of $5x10^{15}$ cm^{-2}. This static model (in which the periodic substrate relaxation was not calculated) kept the substrate unchanged throughout the process and represents a period early in the fin doping PLAD process. In a) only ions implanted into the top corner of the fin were considered, and energetic atoms from their collision cascades, could escape and implant the wall of the opposite fin with sufficient energy to penetrate the surface layer and/or recoil implant deposited As neutrals. Figure 5b) shows that ions directed at one sidewall caused recoil implantation of the deposited As neutral layer with many of the primary ions being reflected and implanted into the bottom of the trench and opposite sidewall. The number of the ions involved in this mechanism depended on the fin sidewall angle. In c) the

ions implanted into the base of the trench sputtered atoms that caused doping in the sidewall, particularly near the fin bottom.

6. Conclusions

Measuring As profiles in planar PLAD samples using MEIS and interpreting the results to give consistency with a TRIDYN model allowed the magnitudes of ion and neutral fluxes occurring during PLAD implants to be estimated. This was very valuable as the fluxes could not be directly measured by the PLAD dosimetry system. The Si profile showed that atoms originating from chamber walls as well as those from the plasma had to be considered.

Dopant profiles in FinFETS extracted from TOF-MEIS spectra appeared to be consistent with a TRI3DYN model using particle flux magnitudes calibrated by the planar results. Comparisons between TRI3DYN results and TEM images gave information on the angular distributions of the neutral particles, which further suggested the importance of accounting for species originating from the chamber walls.

TRIDYN and TRI3DYN modelling has illustrated the relative contributions of direct and recoil implantation during PLAD processing of planar and FinFET structures and given insight into particle scattering mechanisms occurring around 3D structures. All this information should lead to a deeper understanding and improved control of PLAD implantation.

7. Acknowledgements

JE would like to thank the Plasma Doping Group and Hans Gossmann at, Varian Semiconductor Equipment for data, discussions and help in preparing this paper; Pedro Grande, Igor Alencar, Gabriel Marmitt and Henrique Trombini from Universidade Federal do Rio Grande do Sul, Porto Alegre, Brazil for useful discussions, advice and access to POWERMEIS; DaeWon Moon of Daegu Gyeongbuk Institute of Science and Technology for organising the TOF-MEIS measurements.

8. References:

[1] W. Möller and W. Eckstein, Nucl. Instr. And Meth. B2 (1984) 814

[2] W. Möller, Nucl. Instr. And Meth. B322 (2014) 23

[3] T. Miller, L. Godet, G. D. Papasouliotis and V. Singh, AIP Conference Proceedings 1066, (2008) 457

[4] J. Van den Berg, P. Bailey, R. Barlow, T. Noakes, S. Kilcoyne and R. Cywinski, 'The UK MEIS facility: a new future at the IIAA, Huddersfield' in *23rd Conference on Accelerators in Research and Industry, 25-30 May 2014*, San Antonio, Texas, USA

[5] K.-W. Jung, H. Yu, W. J. Min, K.-S. Yu, M. A. Sortica, P. L. Grande, and D. W. Moon, Anal. Chem. 86 (2014) 1091

[6] M. Sortica, P. Grande, G. Machado and L. Miotti, J. Appl. Phys. 106 (2009) 114320

Figure Captions

Figure 1: MEIS energy spectra collected for two samples (random orientation) corresponding to process conditions shown by the TEM images of Figure 2. The highest energy peaks are due to ions that scattered off As atoms. Events below ~77keV are from Si atoms with small peaks from O atoms superimposed around 60keV.

Figure 2: Cross sectional TEM images for samples after a) PLAD and b) PLAD and a wet clean. The black layers on the left side of both images are the Ir caps from the TEM sample preparation. The solid lines with symbols superimposed onto the images show the elemental concentrations and thicknesses of the layers used by POWERMEIS to fit the measured MEIS spectra. The dotted lines show predictions of the TRIDYN model. The images and MEIS measurements were made on different samples that had been processed in the same way.

Figure 3: Cross section TEM images of a FinFET a) before implant, b) post-implant and c) post-anneal with TRI3DYN model predictions overlayed. The solid red contours show where the Si concentration is $3x10^{22}cm^{-3}$ – the positions to where the As was removed to model the wet clean and the oxide removed to model the post anneal DHF step.

Figure 4: Comparison between As profiles a) modelled by TRI3DYN after wet clean and b) post-anneal measured by TOF-MEIS. Boxes show the positions at the fin top and across the sidewall where the dopant distributions are plotted in c) for the top of the fin and d) in the sidewall. In the TRI3DYN profiles the As ions (red dotted lines) should be added to the recoil implanted As neutrals (thin black lines) to compare to the total As measured by MEIS (thick blue lines).

Figure 5: Results of a TRI3DYN model showing As dopant profiles produced part way through a PLAD implant of a FinFET. These profiles correspond to As that originated from a

surface deposition layer and were recoil implanted deeply enough to survive a cleaning step. The boxes above the fins show the regions from where ions were launched vertically downwards towards selected regions of the substrate. The TRI3DYN model illustrates sidewall doping mechanisms caused by As and Xe ions directed at a) part of the fin top, b) left hand sidewall and c) trench bottom.

Figure 1

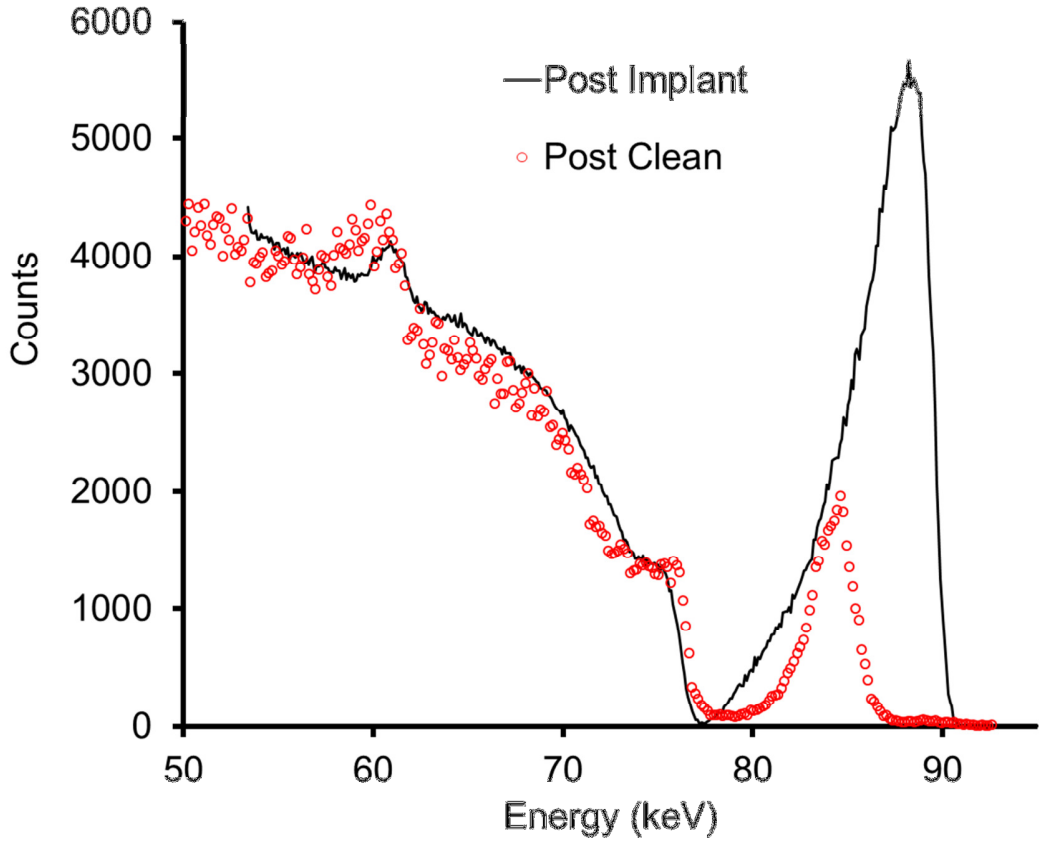
6000
5000
4000
3000
2000
1000
0
Counts
50
60
70
80
90
Energy (keV)
—Post Implant
Post Clean

Figure 2

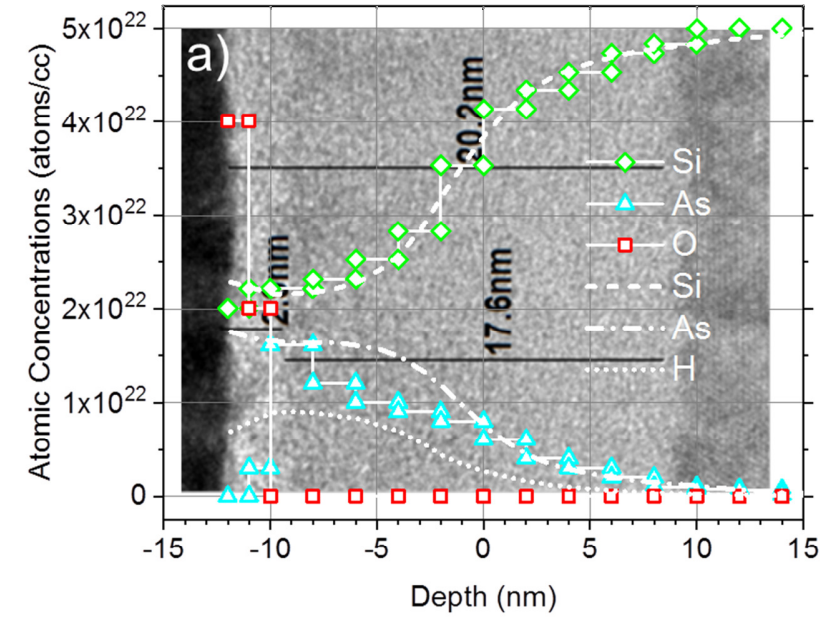
a)
Atomic Concentrations (atoms/cc)
5x10^22
4x10^22
3x10^22
2x10^22
1x10^22
0
-15
-10
-5
0
5
10
15
Depth (nm)
30.2nm
17.6nm
Si
As
O
Si
As
H

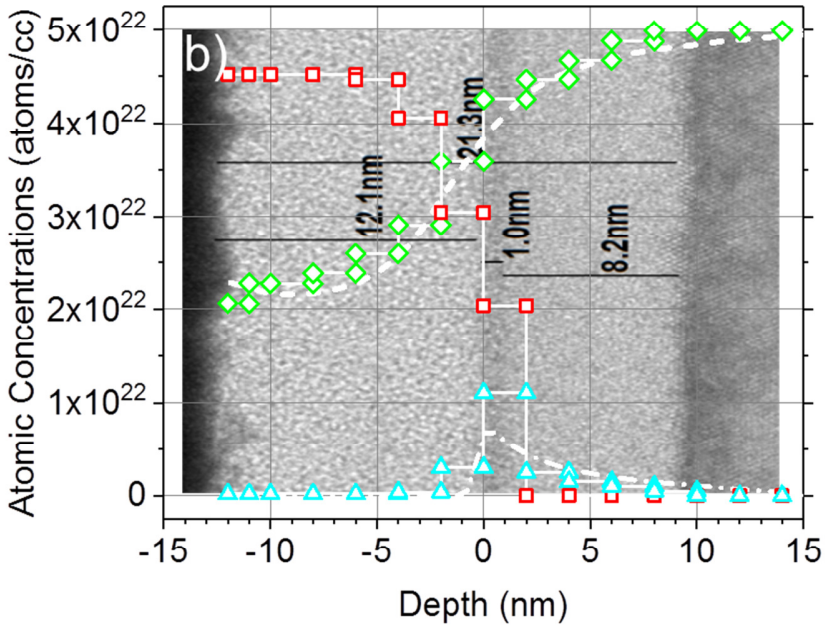
b)
Atomic Concentrations (atoms/cc)
5x10^22
4x10^22
3x10^22
2x10^22
1x10^22
0
-15
-10
-5
0
5
10
15
Depth (nm)
21.3nm
12.1nm
1.0nm
8.2nm

Figure 3

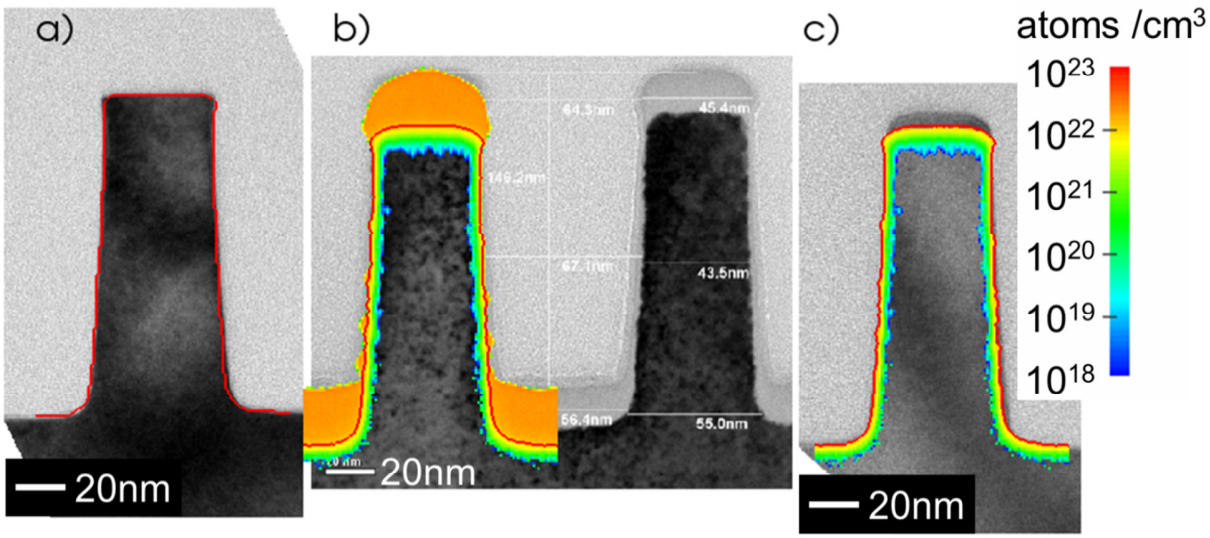
a)
b)
c)
atoms /cm3
10^23
10^22
10^21
10^20
10^19
10^18
20nm
20nm
20nm
64.3nm
45.4nm
149.2nm
67.1nm
43.5nm
56.4nm
55.0nm

Figure 4

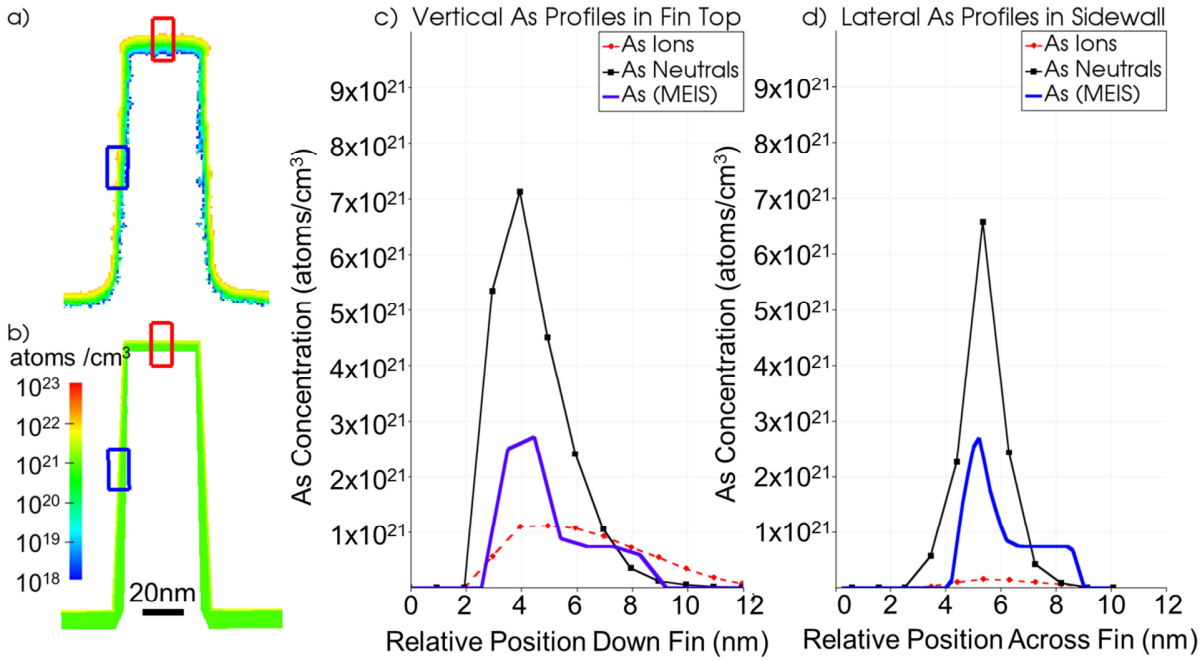
a)
b)
atoms /cm3
10^23
10^22
10^21
10^20
10^19
10^18
20nm
c) Vertical As Profiles in Fin Top
As Ions
As Neutrals
As (MEIS)
As Concentration (atoms/cm3)
9x10^21
8x10^21
7x10^21
6x10^21
5x10^21
4x10^21
3x10^21
2x10^21
1x10^21
0 2 4 6 8 10 12
Relative Position Down Fin (nm)
d) Lateral As Profiles in Sidewall
As Ions
As Neutrals
As (MEIS)
As Concentration (atoms/cm3)
9x10^21
8x10^21
7x10^21
6x10^21
5x10^21
4x10^21
3x10^21
2x10^21
1x10^21
0 2 4 6 8 10 12
Relative Position Across Fin (nm)

Figure 5